

Martens Hardness of CAD/CAM Resin-Based Composites

Martin Rosentritt , Sebastian Hahnel , Sibylle Schneider-Feyrer, Thomas Strasser and Alois Schmid 

Department of Prosthetic Dentistry, UKR University Hospital Regensburg, 93042 Regensburg, Germany; martin.rosentritt@ukr.de (M.R.); sibylle.schneider-feyrer@ukr.de (S.S.-F.); thomas.strasser@ukr.de (T.S.); alois.schmid@ukr.de (A.S.)

* Correspondence: sebastian.hahnel@ukr.de; Tel.: +49-941-944-11900

Abstract: (1) Background: The properties of CAD/CAM resin-based composites differ due to differences in their composition. Instrumented indentation testing can help to analyze these differences with respect to hardness, as well as energy-converting capabilities due to viscoelastic behavior. (2) Methods: Eleven materials were investigated using instrumented indentation testing. Indentation depth (h_r), Martens hardness (H_M), indentation hardness (H_{IT}), indentation modulus (E_{IT}), the elastic part of indentation work (η_{IT}), and indentation creep (C_{IT}) were investigated, and statistical analysis was performed using one-way ANOVA, Bonferroni post-hoc test, and Pearson correlation ($\alpha = 0.05$). (3) Results: All of the investigated parameters revealed differences between the analyzed materials. Besides the differences in hardness-associated parameters (h_r , H_M , and H_{IT}), instrumented indentation testing demonstrated differences in energy-converting properties. The subsequent one-way ANOVA revealed significant differences ($p < 0.001$). A significant ($p < 0.01$, Pearson correlation > 0.576) correlation between the materials and H_M , H_{IT} , or E_{IT} was identified. (4) Conclusions: Due to the differences found in the energy-converting properties of the investigated materials, certain CAD/CAM resin-based composites could show superior stress-breaking capabilities than others. The consequential reduction in stress build-up may prove to be beneficial, especially for implant-retained restorations or patients suffering from parafunctions.



Citation: Rosentritt, M.; Hahnel, S.; Schneider-Feyrer, S.; Strasser, T.; Schmid, A. Martens Hardness of CAD/CAM Resin-Based Composites. *Appl. Sci.* **2022**, *12*, 7698. <https://doi.org/10.3390/app12157698>

Academic Editor: Mary Anne Melo

Received: 11 July 2022

Accepted: 28 July 2022

Published: 30 July 2022

Publisher's Note: MDPI stays neutral with regard to jurisdictional claims in published maps and institutional affiliations.



Copyright: © 2022 by the authors. Licensee MDPI, Basel, Switzerland. This article is an open access article distributed under the terms and conditions of the Creative Commons Attribution (CC BY) license (<https://creativecommons.org/licenses/by/4.0/>).

Keywords: CAD/CAM; resin composite; hardness; instrumented indentation testing

1. Introduction

Due to their clearly deviating properties, resin-based CAD/CAM (computer-aided design/computer-aided manufacturing) composites are an interesting clinical alternative to dental ceramics [1]. Similar to direct resin-based composites, resin-based CAD/CAM composites consist of inorganic fillers embedded in an organic polymer matrix, commonly using silanes as coupling agents. Their mechanical properties such as modulus of elasticity or flexural strength are improved due to the standardized polymerization process under industrial conditions compared to chair-side light-curing polymerization [2]. A variation of resin-based composites is the so-called polymer-infiltrated ceramic network (PICN), which comprises a structure-sintered ceramic matrix and a reinforcing polymer network (ceramic content: 86 wt%; polymer content: 14 wt%). Resin-based CAD/CAM composites and resin-infiltrated ceramic networks are used for inlays, onlays, and veneers, as well as tooth- and implant-retained crowns. Some composites are even approved for bridges and for use in patients suffering from bruxism.

One key benefit of these resin-based materials—as advertised by many manufacturers—is the dentine-like modulus of elasticity of approximately 10–30 GPa. Although composites do not reach the high aesthetics of ceramics, they are commonly regarded as less hard and brittle, and they cause less wear and stress in antagonistic teeth [3]. These qualities may be beneficial for the rehabilitation of patients suffering from parafunctions such as bruxism. Energy-dissipation capabilities might also be increased by the utilization of resin-based CAD/CAM composites with a low modulus of elasticity [4–7]. Implant-supported

restorations, with their lower ductility and elasticity of the osseointegrated implants, might benefit from less stress build-up during normal mastication. For example, there is evidence for improved implant osseointegration with low-modulus titanium implants [8,9]. This phenomena is mostly attributed to the so-called stress-shielding effect, which is caused by the differences of the elastic moduli between implant and bone. The mismatch leads to an insufficient transfer of force and therefore inadequate stimulation of bone remodeling [10]. It is suggested that the stimulation of bone growth may be enhanced by reducing or adjusting the elastic modulus of the restorative material.

Yet, with respect to the mechanical properties of CAD/CAM resin-based composites, previous research suggests a fairly inhomogeneous class of materials [11]. This is mostly attributed to different types, sizes, and amounts of inorganic fillers (approximately 60–85 wt%), as well as the organic matrix [12]. The significant differences in CAD/CAM resin materials, e.g., flexural strength (150–330 MPa) and modulus of elasticity (10.3–30.0 GPa), may have impacts under clinical conditions. To properly evaluate the available materials and perhaps even choose certain materials for specific clinical indications, detailed information on their mechanical behavior is essential. One method for evaluating elastic and viscoelastic behavior is indentation hardness testing. Surface hardness is defined as the resistance against plastic and therefore permanent deformation by indentation. Hardness is commonly measured with methods such as Vickers, Rockwell or Brinell hardness testing. However, indentation testing encompasses more than just permanent deformation, as elastic or even viscoelastic components can also be determined by the measurement. These properties can be measured using instrumented indentation testing, also called Martens hardness (H_M) testing. H_M is derived from the applied force (F) divided by the indentation surface (A_S), which is a function of the indentation depth (h) (Equation (1)).

$$H_M = \frac{F}{A_S(h)} \quad (1)$$

Furthermore, the constant measurement of force and indentation depth provides a force-indentation depth curve, as well as the fundamentals for additional analysis.

The indentation modulus (E_{IT}), which is determined in the compression mode, is related but not identical to the modulus of elasticity, which is determined in the flexure mode [13]. The elastic part of the indentation (expressed by η_{IT}) could help in the assessment of the use of resin-based CAD/CAM composites for use as stress-breakers for implant-supported restorations. The time-dependent response to the indentation of a viscoelastic material [14] can be expressed as indentation creep (C_{IT}), expressing the relative increase of strain under constant force application, e.g., due to the rearrangement of polymer chains. As the deformation caused by creep is of plastic character, C_{IT} can help to estimate the long-term dimensional and mechanical stability of a material [15–18]. Materials that significantly differ in these properties could therefore be used for different applications.

The hypothesis of this study was that different CAD/CAM resin-composite materials show no similarities regarding indentation depth (h_r), Martens hardness (H_M), indentation hardness (H_{IT}), indentation modulus (E_{IT}), the elastic part of indentation work (η_{IT}), and indentation creep (C_{IT}). The obtained results can help to estimate the energy-conversion behavior and therefore the clinical performance of the significantly different materials under masticatory loads, as well as their stress-breaking capabilities.

2. Materials and Methods

Eleven resin-based CAD/CAM materials ($n = 6$ per material) were investigated using instrumented indentation testing according to ISO 14577-1 [19]. Table 1 provides an overview over the tested materials, as well as some of their properties (modulus of elasticity E (GPa), filler content wt. (%), and fracture strength FS (MPa)) for the better interpretation of the results of this study. Rectangular specimens ($10 \times 10 \times 2$ mm) were produced in CAD/CAM dental milling machine (98 milling blank, Inlab MC X5, Dentsply Sirona, Germany) and polished (1000 grit sandpaper, Tegramin 25, Struers, Germany).

Table 1. Materials, manufacturers, abbreviations (Abbr.), modulus of elasticity (E), filler content (wt.), fracture strength (FS) according to manufacturer’s specifications or literature: ^a [20], ^b [21], ^c [22], and ^d [11]). Filler content classification: low-fill $\leq 74\%$ wt. \leq compact.

Material	Manufacturer	Abbr.	E [GPa]	wt. [%] ^d	FS [MPa]
Cerasmart	GC Corp., Tokyo, JP	CS	12.1 ^a	66.9	231
Brilliant Crios	Coltene Holding AG, Altstätten, CH	BC	10.3	72.0	198
Estelite	Tokuyama Dental, Chiyoda, JP	EL	13.8	72.4	225
Block HC	Shofu Dental GmbH, Ratingen, GER	BL	9.5 ^b	64.1	191
Katana Avencia	Kuraray Noritake, Tokyo, JP	KA	12.4	58.6	190
KZR CAD	Yamakin Co. Ltd., Kochi, JP	KC	10.4	69.0	235
Experimental		EX	20.0	78.3	200
Lava Ultimate	3M Deutschland GmbH, Neuss, GER	LU	12.7	75.4	204 ^c
Grandio bloc	VOCO GmbH, Cuxhaven, GER	GB	18.0	84.5	330
VOCO Experimental	VOCO GmbH, Cuxhaven, GER	VO	n/a	79.7	n/a
Vita Enamic	VITA Zahnfabrik, Bad Säckingen, GER	VE	30.0	85.1	150–160

Testing was carried out with a universal hardness-testing machine (ZwickiLine Z2.5, ZwickRoell, Germany; see Figure 1).

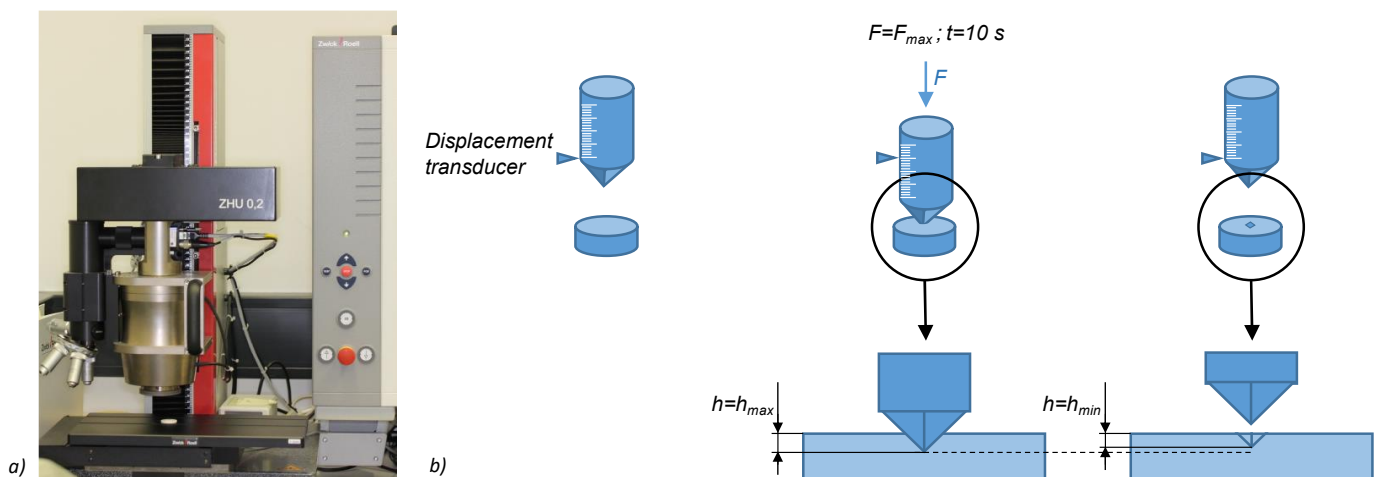


Figure 1. (a) ZwickiLine Z2.5 and (b) schematic test procedure with maximum indentation depth (h_{max}) at application of maximum force (F_{max}) and residual indentation depth (h_{min}) after stress relaxation.

The Martens hardness (H_M) is the ratio of the maximum force to the associated contact area (N/mm^2). Other material parameters, such as indentation modulus, indentation creep, and plastic and elastic work of deformation, can be characterized from a force–indentation depth curve. In this study, force, depth and time during the indentation of the diamond pyramid were continuously recorded. The contact area under load was calculated from the maximum indentation depth. The indentation depth was constantly monitored at a loading speed of 0.5 mm/min to a maximum force of $F_{max} = 10$ N using a Vickers indenter and dwell-time of 10 s. Unloading was performed at 0.1 mm/min. The recorded force–indentation depth curves were used to calculate indentation depth (h_r), Martens hardness (H_M), indentation hardness (H_{IT}), indentation modulus (E_{IT}), the elastic part of indentation work (η_{IT}), and indentation creep (C_{IT}) as defined in ISO 14577-1. The Poisson’s ratio of the diamond indenter was set to $\nu_i = 0.07$, and that of the resin-based composite materials was set to $\nu_s = 0.3$ [23]. The Young’s modulus of the indenter was $E_i = 1140$ GPa.

Calculations and statistical analyses were performed using SPSS 25.0 for Windows (IBM, Armonk, NY, USA). The normal distribution of data was controlled using the Shapiro–Wilk test. Means and standard deviations were calculated and analyzed using ANOVA

and the Bonferroni test for post-hoc analysis. Pearson correlations were calculated. The level of significance was set to $\alpha = 0.05$.

3. Results

The Shapiro–Wilk test confirmed the normal distribution of the tested parameters. The one-way ANOVA revealed significant differences ($p < 0.001$) within the parameters. Table 2 shows mean results and statistical Bonferroni post-hoc comparison. Force–indentation–curves of the investigated materials are shown in Figure 2.

Table 2. Material, abbreviation (Abbr.), mean and standard deviation (in brackets) for indentation depth (h_r), Martens hardness (H_M), indentation hardness (H_{IT}), indentation modulus (E_{IT}), elastic part of indentation work (η_{IT}), and indentation creep (C_{IT}). Identical superscript letters indicate column-wise non-significant (Bonferroni post hoc test, $p > 0.05$) differences between the materials.

Material	Abbr.	h_r [μm]	H_M [N/mm^2]	H_{IT} [N/mm^2]	E_{IT} [kN/mm^2]	η_{IT} [%]	C_{IT} [%]
Cerasmart	CS	22.8 ^{a,b,d,f} (1.7)	441.3 ^{a,b,d,f} (60.1)	688.5 ^{a,b,c,d,f,g} (88.8)	10.2 ^{a,b,d,f,g,h} (1.9)	48.3 ^{a,b,c,d,f,g,h,i,j} (7.0)	4.7 ^{a,b,c,d,e,f,g} (0.5)
Brilliant Crios	BC	22.7 ^{a,b,d,f} (0.5)	438.5 ^{a,b,d,f} (40.4)	689.5 ^{a,b,c,d,f,g} (40.0)	10.0 ^{a,b,d,f,h} (1.6)	44.1 ^{a–k} (2.1)	4.9 ^{a,b,c,d,e,f,g} (0.3)
Estelite	EL	19.4 ^{c,d,e,g,h,j,k} (0.7)	602.8 ^{c,e,g,h,k} (47.9)	940.2 ^{a,b,c,d,e,f,g,h,j,k} (66.8)	13.9 ^{c,f,g} (1.5)	45.2 ^{a–k} (1.6)	4.5 ^{a,b,c,d,e,f,g,j} (0.3)
Block HC	BL	22.1 ^{a,b,c,d,f,g} (0.7)	457.3 ^{a,b,d,f,g,h} (27.4)	724.0 ^{a,b,c,d,f,g} (46.1)	10.2 ^{a,b,d,f,g,h} (0.6)	48.5 ^{a,b,c,d,f,g,h,i,j} (0.7)	4.5 ^{a,b,c,d,e,f,g,h,j} (0.2)
Katana Avencia KZR CAD	KA KC	23.0 ^{a,b,d,f} (1.4) 19.7 ^{c,d,e,g,j,k} (1.6)	410.8 ^{a,b,d,f} (55.8) 584.0 ^{c,d,e,g,j,k} (45.1)	666.5 ^{a,b,c,d,f,g} (88.2) 920.5 ^{a,b,c,d,e,f,g,h,j,k} (141.6)	8.8 ^{a,b,d,f} (1.4) 13.5 ^{a,c,d,g,h} (0.6)	50.0 ^{a,b,c,d,f,g,h,i} (2.3) 45.6 ^{a–k} (7.4)	5.0 ^{a,b,c,d,e,f,g} (0.2) 5.1 ^{a,b,c,d,e,f,g} (0.4)
Experimental	EX	18.7 ^{c,e,g,h,j,k} (0.1)	694.7 ^{c,e,g,h,j,k} (8.5)	1034.5 ^{c,e,g,h,j,k} (12.3)	17.8 ^{e,j,k} (0.3)	40.5 ^{b,c,e,g,j,k} (0.3)	4.8 ^{a,b,c,d,e,f,g} (0.4)
Lava Ultimate	LU	19.1 ^{c,e,g,h,j,k} (3.3)	588.3 ^{c,d,e,g,h,k} (122.6)	1008.7 ^{c,e,g,h,j,k} (331.2)	12.2 ^{a,b,c,d,g,h} (2.2)	50.4 ^{a,b,c,d,f,g,h,i} (4.3)	3.8 ^{d,h,i,j,k} (0.4)
Grandio bloc	GB	17.4 ^{c,e,g,h,j,k} (0.8)	771.2 ^{e,j,k} (73.7)	1184.8 ^{c,e,g,h,j,k} (107.8)	18.4 ^{e,j,k} (2.0)	42.7 ^{a,b,c,d,e,g,i,j,k} (1.5)	4.0 ^{c,d,h,j,k} (0.2)
VOCO Experimental	VO	18.7 ^{c,e,g,h,j,k} (0.3)	692.0 ^{c,e,g,h,j,k} (212.0)	1036.8 ^{c,e,g,h,j,k} (32.3)	17.5 ^{e,j,k} (0.8)	40.2 ^{b,c,e,g,j,k} (0.5)	3.8 ^{h,i,j,k} (0.2)
Vita Enamic	VE	13.9 (0.7)	1143.3 (124.7)	1834.2 (198.0)	25.3 (3.0)	49.2 ^{a,b,c,d,f,g,h,i,j} (0.7)	3.2 ^{h,i,k} (0.1)

The mean Martens hardness (H_M) ranged from $410.8 \pm 55.8 \text{ N}/\text{mm}^2$ (KA) to $1143.4 \pm 124.7 \text{ N}/\text{mm}^2$ (VE). The ANOVA showed significant ($p \leq 0.001$) differences between the results (Table 2). The residual indentation depth (h_r) was between $13.9 \pm 0.7 \mu\text{m}$ (VE) and $23.0 \pm 1.4 \mu\text{m}$ (KA), with significant differences between the results (ANOVA: $p \leq 0.001$). The indentation hardness (H_{IT}) varied between $666.5 \pm 88.2 \text{ N}/\text{mm}^2$ (KA) and $1834.2 \pm 198.0 \text{ N}/\text{mm}^2$ (VE). The ANOVA confirmed significant ($p \leq 0.001$) differences between the results. The indentation modulus (E_{IT}) ranged from $8.8 \pm 1.4 \text{ kN}/\text{mm}^2$ (KA) to $25.3 \pm 3.0 \text{ kN}/\text{mm}^2$ (VE), with significant differences between the results (ANOVA: $p \leq 0.001$). The mean elastic part of indentation (η_{IT}) varied between $40.2 \pm 0.5\%$ (VO) and $50.4 \pm 4.3\%$ (LU) (Figure 3). The ANOVA confirmed significant differences between the mean values ($p \leq 0.001$). The indentation creep (C_{IT}) ranged from $3.2 \pm 0.1\%$ (VE) to $5.1 \pm 0.4\%$ (KC). The ANOVA showed significant ($p \leq 0.001$) differences between the values.

A highly significant ($p < 0.01$, Pearson correlation >0.576) correlation between the materials and H_M , H_{IT} or E_{IT} was identified. Negative correlations were established for h_r (-0.623), and C_{IT} (-0.584). No correlation could be determined for η_{IT} (-0.151 , $p = 0.227$). A significant ($p < 0.001$) impact of the material was found on H_M ($\eta^2 = 0.914$), H_{IT} ($\eta^2 = 0.867$), E_{IT} ($\eta^2 = 0.910$), C_{IT} ($\eta^2 = 0.771$), η_{IT} ($\eta^2 = 0.544$), and h_r ($\eta^2 = 0.814$).

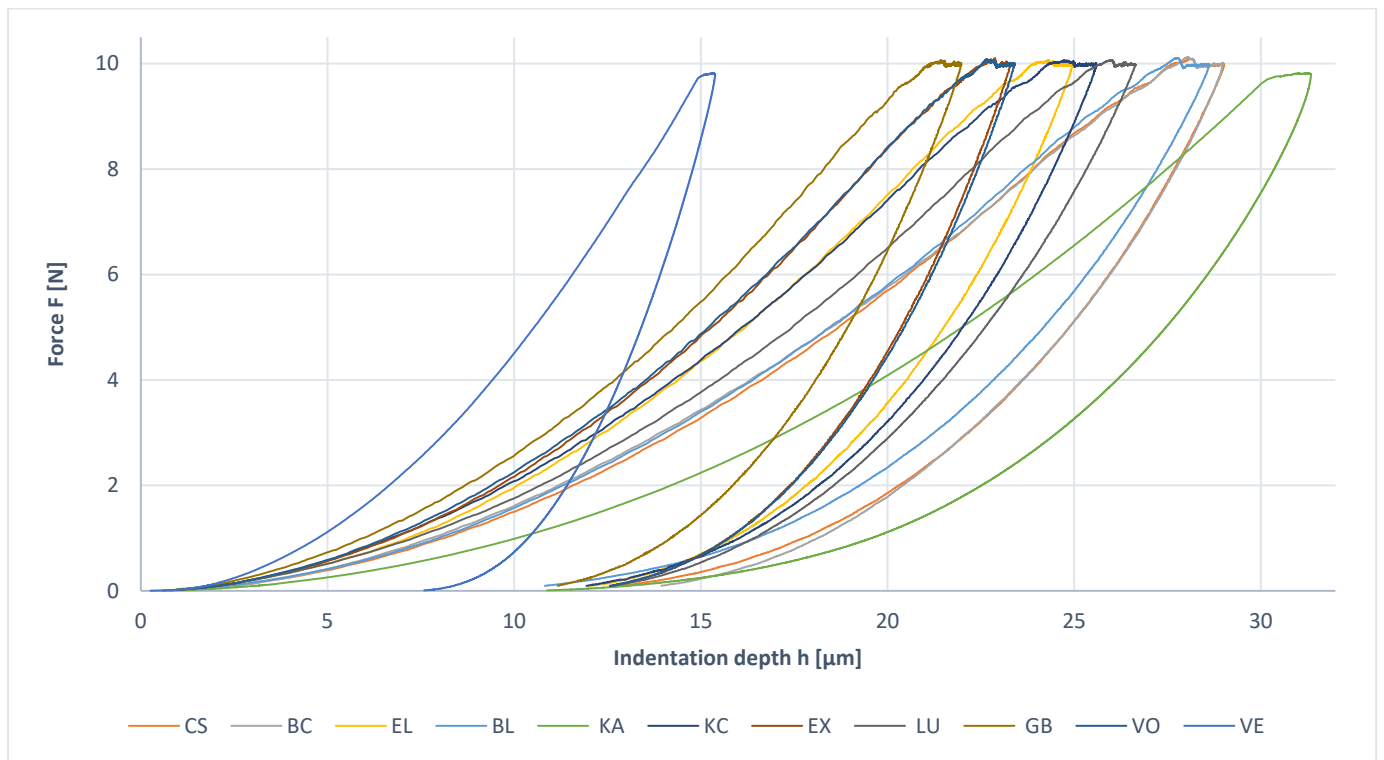


Figure 2. Force-indentation depth curves of the tested composite materials.

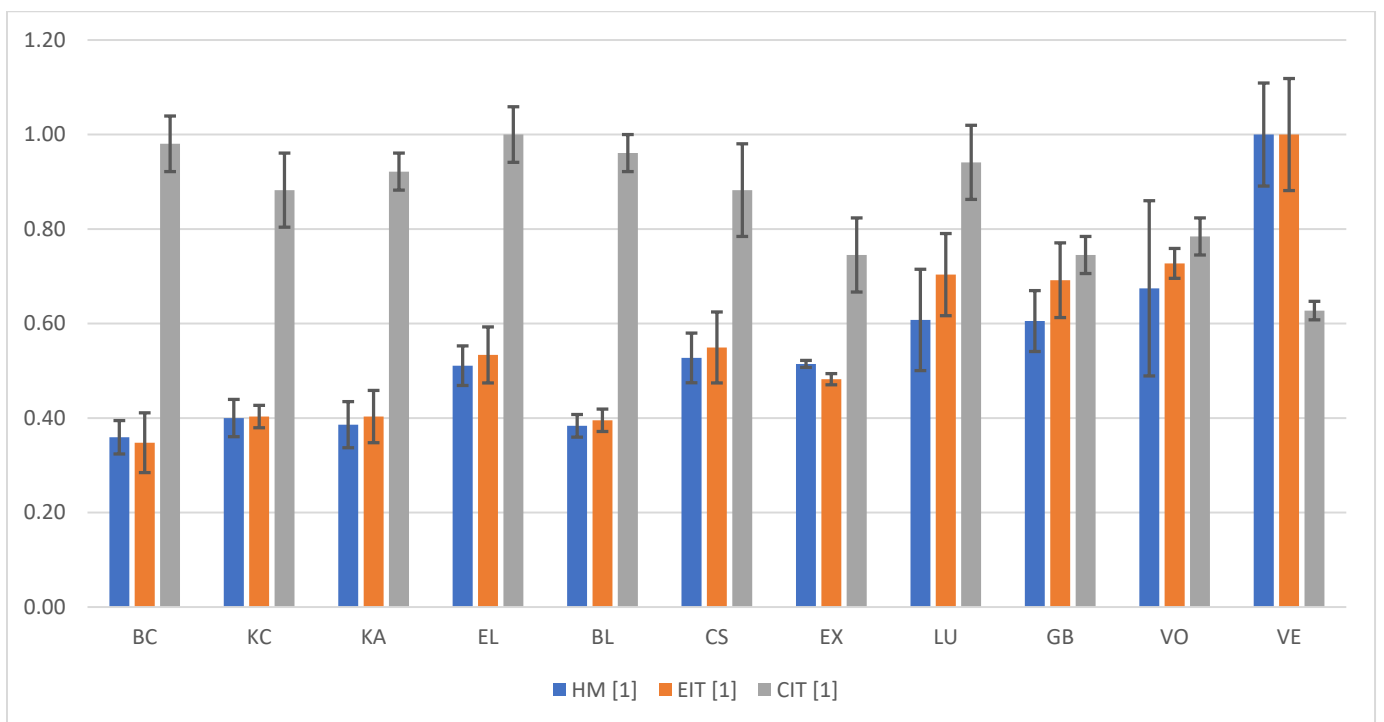


Figure 3. Martens hardness (H_M), indentation modulus (E_{IT}), and indentation creep (C_{IT}) scaled to percentage of maximum value. Materials ordered by increasing amount of inorganic filler content.

4. Discussion

The hypothesis that different CAD/CAM resin-composite materials show no similarities regarding indentation depth (h_T), Martens hardness (H_M), indentation hardness (H_{IT}), indentation modulus (E_{IT}), the elastic part of indentation work (η_{IT}), and indentation

creep (C_{IT}) could be partly confirmed. The novelty of this study is that the data were used not only to evaluate the material hardness but also to differentiate the elastic and viscoelastic surface parameters. In addition, possible clinical consequences of the results and applications were discussed.

Figure 4 shows the force–indentation depth curves, which highlight individual parameters investigated in this study. In comparison to research on the Martens hardness of CAD/CAM resin-based materials, the published H_M values for the PICN material (VE) are distinctly higher (1524–1555 N/mm^2) compared to the results of this investigation (1143 N/mm^2) [24,25]. Differences here were due to the transverse contraction number required for the calculations. With respect to the resin-composite materials with a filler content of more than 70%, the H_M values found in the literature (667–1089 N/mm^2) are in line or above the results of this study (588–771 N/mm^2) [24–27]. The H_M values reported in the literature for composites with a filler content below 70% are distinctly below (BC*: 151 N/mm^2) [24] or in line (477–573 N/mm^2) [25,27] with the values obtained in this investigation (411–603 N/mm^2). The E_{IT} values found in the literature (2.5–30 kN/mm^2) are lower or in line with the results of this study (9–25 kN/mm^2) [24]. The C_{IT} values obtained in this study (3.2–5.1%) were slightly higher compared to those of the literature (2.6–3.4%) [26,27].

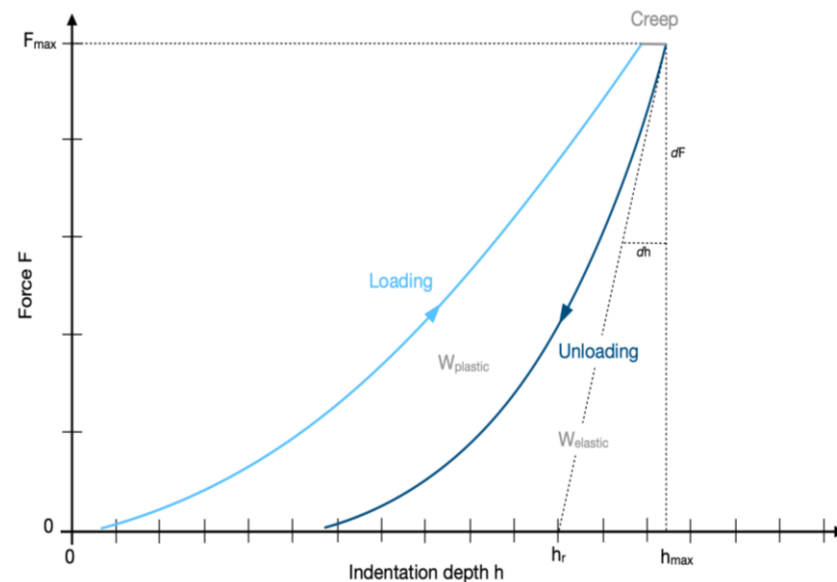


Figure 4. Showcase force–indentation depth curve. $W_{plastic/elastic}$ = plastic/elastic indentation work; dF/dh = contact stiffness S ; F_{max} = maximum force; h_{max} = maximum indentation depth; h_r = depth at contact stiffness tangent.

Creep and therefore C_{IT} values are characterized by the short horizontal parts of a depth curve at peak force. E_{IT} values are determined by the slope of the ascending part of the curve. The curve of VE indicates low C_{IT} and high E_{IT} values, which indicates a low susceptibility to creep and high resistance against elastic deformation. The curve of KA in comparison shows a longer horizontal movement at peak force and a less steep slope of the ascending curve, indicating higher C_{IT} and lower E_{IT} values. In this study, the H_M values started at about 400 N/mm^2 for the composite with the lowest filler content and were almost twice as high for the composite with the highest filler content. Three times higher values were even identified for PICN, although the inorganic weight content was slightly comparable to that of the highly filled composite. These results confirm previous research that indicated a positive correlation between inorganic filler content and surface hardness for resin-based composites [28–30]. However, our results also confirm the special position of PICN [24,31]. As expected, a comparable behavior was also observed for results of h_r , with an approximately 25% lower indentation depth for the highly filled composite or

even 40% for the PICN. However, there were also exceptions in the resin-based composite group, since, e.g., materials with the same filler content (BC and ES; approximately 72%) showed differences of up to 25%. Filler type and size, as well as polymer composition or the chemical bonding of the fillers, may also affect materials' surface properties and explain the differences in materials with similar filler contents [12,32–34]. A correlation between surface hardness and inorganic filler content [11] could also be observed for the materials investigated in this study. The relative differences in standard deviations can be attributed to the uneven filler distribution and the resulting different filler content on the material surface. Since the composition and topography of a material's surface have decisive influence on hardness measurements, results may vary accordingly. In addition, a different polymerization of the matrix due to a distinct manufacturing process can influence results [27]. Resin-composite materials are considered to be less hard and brittle and to cause less stress build-up in antagonistic teeth compared to ceramics. The present material's properties were within the range of data of human dentine from literature (indentation hardness of 0.4–1.1 GPa and indentation modulus of 12.2–22.9 GPa) [35–37]. As the elastic modulus also resembles that of dentin (approximately 15 GPa) [38], CAD/CAM composites could be considered when looking for a biomimetic approach for a dentine replacement [39].

With mean indentation creep C_{IT} values between 3.2% and 5.1%, the analyzed resin composite materials were more resistant to creep compared to human dentine at 8.6 to 10.7% [37]. However, C_{IT} is difficult to interpret in the context of dental materials and their clinical application, as the duration of teeth contact in a physiological masticatory cycle is only about 0.1 to 0.2 s [40], whereas the application time is 10 s during instrumented indentation testing. Assuming only intermittent tooth contact, e.g., while chewing or swallowing, as well as the natural energy-dissipation capabilities of hard dental tissues and the periodontal ligament, the differences in C_{IT} seem to be negligible. However, clenching or bruxism, perhaps even in combination with reduced resiliency in implants or ankylosed teeth, could increase the significance of creep behavior because the magnitude and, especially, the duration of stress application may increase. In these cases, creep will be more relevant for the long-term stability and integrity of the restoration, as stress will also be induced at the intaglio surface [41,42]. This phenomena could lead to debonding, permanent deformation, and perhaps ultimately to an insufficient fit of the restoration. At the tooth–restoration interface, creep could lead to over-contouring or the formation of gaps, which could significantly reduce clinical performance. The energy-dissipating capabilities (“damping effects”) are associated with the conversion of energy (storage and energy dissipation). The obtained η_{IT} values indicate the work that is converted into potentially stored elastic energy ($w_{elastic}$), whereas the other part of indentation work is mostly dissipated throughout plastic deformation or heat ($w_{plastic}$).

Based on the current data, an indication-driven selection of the investigated materials could improve clinical performance. For example, the reduced resiliency and tactility of implants could be compensated for by a material that causes less stress build while being creep resistant. Such a material must therefore have low E_{IT} and C_{IT} values. The finite element analysis of inlay or partial crowns with higher elastic moduli points to higher stress build-up within the restoration while simultaneously causing less stress build-up in the cement layer and hard dental tissue [43–45]. Materials with high E_{IT} and fracture strength values yet low C_{IT} values could therefore show superior clinical performance when used for partial or inlay crowns. Materials with high C_{IT} values should be considered with caution for permanent restorations. However, the ability to gradually deform under constant stress could be useful in cases where a certain self-balancing effect is desired. These materials could therefore be considered for long-term temporary crowns during pre-prosthetic treatment, as the viscoelastic behavior could help to self-equilibrate the occlusion. The parameters presented in this study can be regarded as a relevant contribution to established parameters such as flexural strength, wear, and filler content.

5. Conclusions

The authors of this study investigated the mechanical properties (indentation depth (h_r), Martens hardness (H_M), indentation hardness (H_{IT}), indentation modulus (E_{IT}), elastic part of indentation work (η_{IT}), and indentation creep (C_{IT})) of CAD/CAM resin-based composites with instrumented indentation testing. The Martens hardness and energy-conversion capabilities of eleven different CAD/CAM composites were investigated with a reference to clinical application. Within the limitations of this study, the following conclusions can be drawn:

- The clinical behavior of dental restorations can be influenced by selecting materials based on different elastic and viscoelastic surface parameters.
- Hardness, indentation modulus, and creep vary significantly between different CAD/CAM resin-based composites.
- Individual CAD/CAM resin-composites show different stress-breaking capacities for implant-retained crowns. The reduced resiliency and tactility of implants might be compensated for by a material with low E_{IT} and C_{IT} values.
- Materials with high E_{IT} and low C_{IT} values might be beneficial for partial or inlay crown applications.

Author Contributions: Conceptualization and writing—review and editing, M.R.; writing—review and editing, S.H.; investigation and data curation, S.S.-F.; writing—review and editing, T.S.; writing—original draft preparation, A.S. All authors have read and agreed to the published version of the manuscript.

Funding: This research received no external funding.

Institutional Review Board Statement: Not applicable.

Informed Consent Statement: Not applicable.

Data Availability Statement: Data are contained within the article.

Acknowledgments: We thank the manufacturers for providing the investigated materials.

Conflicts of Interest: The authors declare no conflict of interest.

References

1. Miura, S.; Fujisawa, M. Current status and perspective of CAD/CAM-produced resin composite crowns: A review of clinical effectiveness. *Jpn. Dent. Sci.* **2020**, *56*, 184–189. [[CrossRef](#)] [[PubMed](#)]
2. Alt, V.; Hannig, M.; Wöstmann, B.; Balkenhol, M. Fracture strength of temporary fixed partial dentures: CAD/CAM versus directly fabricated restorations. *Dent. Mater.* **2011**, *27*, 339–347. [[CrossRef](#)] [[PubMed](#)]
3. Ruse, N.D.; Sadoun, M.J. Resin-composite Blocks for Dental CAD/CAM Applications. *J. Dent. Res.* **2014**, *93*, 1232–1234. [[CrossRef](#)] [[PubMed](#)]
4. Skalak, R. Biomechanical considerations in osseointegrated prostheses. *J. Prosthet. Dent.* **1983**, *49*, 843–848. [[CrossRef](#)]
5. Rohr, N.; Coldea, A.; Zitzmann, N.U.; Fischer, J. Loading capacity of zirconia implant supported hybrid ceramic crowns. *Dent. Mater.* **2015**, *31*, e279–e288. [[CrossRef](#)] [[PubMed](#)]
6. Rosentritt, M.; Schneider-Feyrer, S.; Behr, M.; Preis, V. In Vitro Shock Absorption Tests on Implant-Supported Crowns: Influence of Crown Materials and Luting Agents. *Int. J. Oral. Maxillofac. Implants* **2017**, *33*, 116–122. [[CrossRef](#)] [[PubMed](#)]
7. Niem, T.; Gonschorek, S.; Wöstmann, B. New method to differentiate surface damping behavior and stress absorption capacities of common CAD/CAM restorative materials. *Dent. Mater.* **2021**, *37*, e213–e230. [[CrossRef](#)]
8. Shi, L.; Wang, L.; Duan, Y.; Lei, W.; Wang, Z.; Li, J.; Fan, X.; Li, X.; Li, S.; Guo, Z. The Improved Biological Performance of a Novel Low Elastic Modulus Implant. *PLoS ONE* **2013**, *8*, e55015. [[CrossRef](#)] [[PubMed](#)]
9. Brizuela, A.; Climent, M.; Rios-Carrasco, E.; Rios-Santos, J.; Perez, R.; Manero, J.M.; Gil, F.J. Influence of the Elastic Modulus on the Osseointegration of Dental Implants. *Materials* **2019**, *12*, 980. [[CrossRef](#)] [[PubMed](#)]
10. Zhang, Y.; Wang, J.; Wang, P.; Fan, X.; Li, X.; Fu, J.; Li, S.; Fan, H.; Guo, Z. Low elastic modulus contributes to the osteointegration of titanium alloy plug. *J. Biomed. Mater. Res. Part. B Appl. Biomater.* **2013**, *101*, 584–590. [[CrossRef](#)]
11. Rosentritt, M.; Schneider-Feyrer, S.; Strasser, T.; Koenig, A.; Schmohl, L.; Schmid, A. Thermoanalytical Investigations on the Influence of Storage Time in Water of Resin-Based CAD/CAM Materials. *Biomedicines* **2021**, *9*, 1779. [[CrossRef](#)] [[PubMed](#)]

12. Rosentritt, M.; Huber, C.; Strasser, T.; Schmid, A. Investigating the mechanical and optical properties of novel Urethandimethacrylate (UDMA) and Urethanmethacrylate (UMA) based rapid prototyping materials. *Dent. Mater.* **2021**, *37*, 1584–1591. [[CrossRef](#)] [[PubMed](#)]
13. Oliver, W.C.; Pharr, G.M. An improved technique for determining hardness and elastic modulus using load and displacement sensing indentation experiments. *J. Mater. Res.* **1992**, *7*, 1564–1583. [[CrossRef](#)]
14. Shahdad, S.A.; McCabe, J.F.; Bull, S.; Rusby, S.; Wassell, R.W. Hardness measured with traditional Vickers and Martens hardness methods. *Dent. Mater.* **2007**, *23*, 1079–1085. [[CrossRef](#)] [[PubMed](#)]
15. Baroudi, K.; Silikas, N.; Watts, D.C. Time-dependent visco-elastic creep and recovery of flowable composites. *Eur. J. Oral. Sci.* **2007**, *115*, 517–521. [[CrossRef](#)]
16. Singh, V.; Misra, A.; Parthasarathy, R.; Ye, Q.; Park, J.; Spencer, P. Mechanical properties of methacrylate-based model dentin adhesives: Effect of loading rate and moisture exposure. *J. Biomed. Mater. Res. B Appl. Biomater.* **2013**, *101*, 1437–1443. [[CrossRef](#)] [[PubMed](#)]
17. Wang, X.; Zhou, J.; Kang, D.; Swain, M.V.; Menčík, J.; Jian, Y.; Zhao, K. The bulk compressive creep and recovery behavior of human dentine and resin-based dental materials. *Dent. Mater.* **2020**, *36*, 366–376. [[CrossRef](#)] [[PubMed](#)]
18. Iwasaki, T.; Kamiya, N.; Hirayama, S.; Tanimoto, Y. Evaluation of the mechanical behavior of bulk-fill and conventional flowable resin composites using dynamic micro-indentation. *Dent. Mater. J.* **2022**, *41*, 87–94. [[CrossRef](#)]
19. *ISO 14577-1; 2002: Metallic Materials—Instrumented Indentation Test for Hardness and Materials Parameters—Part 1: Test method.* ISO: Geneva, Switzerland, 2002.
20. Wendler, M.; Belli, R.; Petschelt, A.; Mevec, D.; Harrer, W.; Lube, T.; Danzer, R.; Lohbauer, U. Chairside CAD/CAM materials. Part 2: Flexural strength testing. *Dent. Mater.* **2017**, *33*, 99–109. [[CrossRef](#)] [[PubMed](#)]
21. Lauvahutanon, S.; Takahashi, H.; Shiozawa, M.; Iwasaki, N.; Asakawa, Y.; Oki, M.; Finger, W.J.; Arksornnukit, M. Mechanical properties of composite resin blocks for CAD/CAM. *Dent. Mater. J.* **2014**, *33*, 705–710. [[CrossRef](#)]
22. Alamouh, R.A.; Silikas, N.; Salim, N.A.; Al-Nasrawi, S.; Satterthwaite, J.D. Effect of the Composition of CAD/CAM Composite Blocks on Mechanical Properties. *BioMed Res. Int.* **2018**, *2018*, 4893143. [[CrossRef](#)] [[PubMed](#)]
23. Choi, B.-J.; Yoon, S.; Im, Y.-W.; Lee, J.-H.; Jung, H.-J.; Lee, H.-H. Uniaxial/biaxial flexure strengths and elastic properties of resin-composite block materials for CAD/CAM. *Dent. Mater.* **2019**, *35*, 389–401. [[CrossRef](#)] [[PubMed](#)]
24. Hampe, R.; Lümekemann, N.; Sener, B.; Stawarczyk, B. The effect of artificial aging on Martens hardness and indentation modulus of different dental CAD/CAM restorative materials. *J. Mech. Behav. Biomed. Mater.* **2018**, *86*, 191–198. [[CrossRef](#)] [[PubMed](#)]
25. Hampe, R.; Theelke, B.; Lümekemann, N.; Stawarczyk, B. Impact of artificial aging by thermocycling on edge chipping resistance and Martens hardness of different dental CAD-CAM restorative materials. *J. Prosthet. Dent.* **2021**, *125*, 326–333. [[CrossRef](#)] [[PubMed](#)]
26. Ilie, N. Altering of optical and mechanical properties in high-translucent CAD-CAM resin composites during aging. *J. Dent.* **2019**, *85*, 64–72. [[CrossRef](#)] [[PubMed](#)]
27. Ilie, N. Spatial Distribution of the Micro-Mechanical Properties in High-Translucent CAD/CAM Resin-Composite Blocks. *Materials* **2020**, *13*, 3352. [[CrossRef](#)] [[PubMed](#)]
28. Li, Y.; Swartz, M.L.; Phillips, R.W.; Moore, B.K.; Roberts, T.A. Effect of filler content and size on properties of composites. *J. Dent. Res.* **1985**, *64*, 1396–1401. [[CrossRef](#)] [[PubMed](#)]
29. Kim, K.-H.; Ong, J.L.; Okuno, O. The effect of filler loading and morphology on the mechanical properties of contemporary composites. *J. Prosthet. Dent.* **2002**, *87*, 642–649. [[CrossRef](#)] [[PubMed](#)]
30. Bociog, K.; Szczesio, A.; Krasowski, M.; Sokolowski, J. The influence of filler amount on selected properties of new experimental resin dental composite. *Open Chem.* **2018**, *16*, 905–911. [[CrossRef](#)]
31. Randolph, L.D.; Palin, W.M.; Leloup, G.; Leprince, J.G. Filler characteristics of modern dental resin composites and their influence on physico-mechanical properties. *Dent. Mater.* **2016**, *32*, 1586–1599. [[CrossRef](#)] [[PubMed](#)]
32. Stöckl, C.; Hampe, R.; Stawarczyk, B.; Haerst, M.; Roos, M. Macro- and microtopographical examination and quantification of CAD-CAM composite resin 2- and 3-body wear. *J. Prosthet. Dent.* **2018**, *120*, 537–545. [[CrossRef](#)] [[PubMed](#)]
33. Yano, H.T.; Ikeda, H.; Nagamatsu, Y.; Masaki, C.; Hosokawa, R.; Shimizu, H. Correlation between microstructure of CAD/CAM composites and the silanization effect on adhesive bonding. *J. Mech. Behav. Biomed. Mater.* **2020**, *101*, 103441. [[CrossRef](#)] [[PubMed](#)]
34. Koenig, A.; Schmidtke, J.; Schmohl, L.; Schneider-Feyrer, S.; Rosentritt, M.; Hoelzig, H.; Kloess, G.; Vejjasilpa, K.; Schulz-Siegmund, M.; Fuchs, F.; et al. Characterisation of the Filler Fraction in CAD/CAM Resin-Based Composites. *Materials* **2021**, *14*, 1986. [[CrossRef](#)] [[PubMed](#)]
35. Halgaš, R.; Dusza, J.; Kaiferova, J.; Kovacsova, L.; Markovska, N. Nanoindentation testing of human enamel and dentin. *Cerami Silik* **2013**, *57*, 92–99.
36. Sadyrin, E.; Swain, M.; Mitrin, B.; Rzhepakovsky, I.; Nikolaev, A.; Irkha, V.; Yogina, D.; Lyanguzov, N.; Maksyukov, S.; Aizikov, S. Characterization of Enamel and Dentine about a White Spot Lesion: Mechanical Properties, Mineral Density, Microstructure and Molecular Composition. *Nanomaterials* **2020**, *10*, 1889. [[CrossRef](#)]
37. Kucher, M.; Dannemann, M.; Modler, N.; Bernhard, M.R.; Hannig, C.; Weber, M.T. Mapping of the Micro-Mechanical Properties of Human Root Dentin by Means of Microindentation. *Materials* **2021**, *14*, 505. [[CrossRef](#)] [[PubMed](#)]
38. Rees, J.S.; Jacobsen, P.H. The elastic moduli of enamel and dentine. *Clinic. Mater.* **1993**, *14*, 35–39. [[CrossRef](#)]

39. Güth, J.F.; Edelhoff, D.; Goldberg, J.; Magne, P. CAD/CAM Polymer vs Direct Composite Resin Core Buildups for Endodontically Treated Molars Without Ferrule. *Oper. Dent.* **2016**, *41*, 53–63. [[CrossRef](#)]
40. Bates, J.F.; Stafford, G.D.; Harrison, A. Masticatory function—A review of the literature. 1. The form of the masticatory cycle. *J. Oral. Rehabil.* **1975**, *2*, 281–301. [[CrossRef](#)]
41. Duan, Y.; Griggs, J.A. Effect of elasticity on stress distribution in CAD/CAM dental crowns: Glass ceramic vs. polymer–matrix composite. *J. Dent.* **2015**, *43*, 742–749. [[CrossRef](#)] [[PubMed](#)]
42. Zheng, Z.; He, Y.; Ruan, W.; Ling, Z.; Zheng, C.; Gai, Y.; Yan, W. Biomechanical behavior of endocrown restorations with different CAD-CAM materials: A 3D finite element and in vitro analysis. *J. Prosthet. Dent.* **2021**, *125*, 890–899. [[CrossRef](#)] [[PubMed](#)]
43. Dejak, B.; Mlotkowski, A.; Langot, C. Three-dimensional finite element analysis of molars with thin-walled prosthetic crowns made of various materials. *Dent. Mater.* **2012**, *28*, 433–441. [[CrossRef](#)] [[PubMed](#)]
44. Costa, A.K.F.; Xavier, T.A.; Noritomi, P.Y.; Saavedra, G.; Borges, A.L.S. The Influence of Elastic Modulus of Inlay Materials on Stress Distribution and Fracture of Premolars. *Oper. Dent.* **2014**, *39*, E160–E170. [[CrossRef](#)] [[PubMed](#)]
45. Özkir, S.E. Effect of restoration material on stress distribution on partial crowns: A 3D finite element analysis. *J. Dent. Sci.* **2018**, *13*, 311–317. [[CrossRef](#)] [[PubMed](#)]